Interfacial reactions between thin metal films and polar {0001} oriented CdS substrates

Part I *Aluminium films on CdS*

E. K. CHIEH, Z. A. MUNIR
Division of Materials Science and Engineering, University of California, Davis, CA 95616, USA

The interaction between deposited Al films on opposite polar {0001} surfaces of CdS single crystals was investigated by Auger electron spectroscopy. Aluminium reacts strongly with CdS resulting in a chemical shift of the Al Auger peaks. A chemical drawing effect is believed to dominate with thinner films, while a chemical trapping effect is dominant with thicker films. A sharp boundary between Al and CdS was formed initially; however, due to the reactive outdiffusion, the boundary became extended (over tens of nanometres) with time. A possible mechanism is proposed to explain these observations. The behaviour of the two polar surfaces of CdS was virtually the same.

1. Introduction

Bonding across a metal–semiconductor interface and formation of a new compound with different work function lead to a local charge redistribution and hence to the creation of a dipole voltage. The sign and the magnitude of this local dipole are determined by the chemical interaction on an atomic level between the metal and the semiconductor. In the case of an interface between a less reactive metal and a semiconductor, strong chemical reactions do not occur but interdiffusion of metal and semiconductor components can take place, extending the charge redistribution away from the initial interface and creating interface-specific states. The type and position of these interface-specific states strongly depend on the detailed movement of the atomic species [1].

Cation and anion concentrations within metal overlayers on III–V and II–VI compound semiconductors depend both on the interface electric dipole induced by the metal chemisorption and the metal-anion bond strength [2]. Dipole voltages (~ 0.1–0.3 eV) set up across only a few tenths of nanometres at the metal–semiconductor interface can produce extremely high electric field gradients ($\sim 10^7 \, \mathrm{V \, cm^{-1}}$) which can enhance or retard ionic motion near the interface. Dipole voltages between various metals and CdS substrates have been measured by Brillson et al. [3–6]. For Al on CdS $(1\,0\,\bar{1}\,0)$, the semiconductor–metal dipole is 0.21 eV and is positive (i.e. the surface is positive relative to the layers below) [3], consistent with electron transfer from Al to the CdS substrate. For Cu on CdS $(1\,0\,\bar{1}\,0)$, the interface dipole layer has a magnitude of 0.2 eV and is negative [4] while the interface dipole for Cu on CdS $(1\,1\,\bar{2}\,0)$ is 0.6 eV and is also negative [5]. Au on CdS $(1\,0\,\bar{1}\,0)$, gives rise to negative dipole of magnitude 0.25 eV [6]. Similarly, Au on CdS $(1\,1\,\bar{2}\,0)$ produced a comparable dipole of 0.3 eV.

Chemical reactions between metals and semicon-ductors at room temperature have been reported for III–V and II–VI compound semiconductors. Brillson [7] has related the interface behaviour to the semiconductor enthalpy of formation. Experiments on both a microscopic and macroscopic scale also revealed that metals deposited on semiconductor surfaces give rise to outdiffusion of semiconductor atoms through the metal. The strength and nature of interfacial chemical bonding has a dramatic effect on the stoichiometry of atomic outdiffusion [8]. In general, the larger the heat of interface reaction, the stronger the anion attenuation rate, and the stronger the "chemical trapping" effect in the metal overlayer.

The crystal structure of CdS in its wurtzite modification is such that alternate {0001} layers in the wurtzite structure of CdS are composed exclusively of Cd and S, with each layer arranged in a close packed manner. The atomic packing leads to a small intrinsic distribution of dipoles with positive orientation on the Cd surface and with negative orientation on the S surface [9]. In the bulk of the CdS crystal, the defects are believed to be Schottky–Wagner type disorder [10, 11], where the predominant defects are charged cation and anion vacancies. However, conductivity measurements on non-stoichiometric CdS have shown that this compound is an n-type semiconductor with a resistivity of 1–10 Ω cm at room temperature, leading to the conclusion that the dominant lattice defects are charged S vacancies [12]. The presence of positively charged S vacancies near the surface of the crystal creates a Debye–Hückel distribution [13] with a negative orientation, i.e. the surface possesses a negative charge with respect to the underlying space charge.

Because the opposite dipole orientation derived from the crystal structure is independent of the Debye–Hückel distribution, the net effect produced by summing the dipole fields is an increase in the total field strength at the S (B) surface and a decrease in the

total field strength at the Cd (A) surface [9, 14]. Thus, for polar $\{0\,0\,0\,1\}$ surfaces, the interface dipole voltage is expected to be smaller or more negative on the S (B) face than on the Cd (A) face.

In this study, a reactive metal, Al, was selected as an overlayer on the polar surfaces, $(0\,0\,0\,1)$ and $(0\,0\,0\,\bar{1})$, of CdS single crystals. In a second paper [15] we report the results of a similar investigation on a less reactive metal (Cu) and an inert metal (Au).

2. Experimental procedure

Cadmium sulphide single crystals of ultra-high purity were used in this research. The crystals were 2 mm thick irregularly shaped wafers with nominal resistivities in the range of 1–10 Ω cm. The crystals were pre-oriented along the c-axis and cut into wafers with large surfaces parallel to the basal plane. The polar $(0\,0\,0\,1)$ and $(0\,0\,0\,\bar{1})$ surfaces were identified by a chemical etch technique [16]. When etched, the Cd face showed characteristic hexagonal etch pits [17] while the S face exhibited non-distinct hillocks interspersed by narrow valleys. Each crystal was cut into two pieces which were mounted side by side on a sample holder such that opposite polarities were facing up. The crystals were then successively polished by using 600 grit sand paper, ~ 0.3 and 0.05 μm Al_2O_3 powder on Buehler microcloth. After polishing and cleaning, the crystals were transferred to a sample stud and loaded into the vacuum system.

The vacuum system is divided into an evaporation chamber and an analysis chamber with a gate valve connecting the two. A turbomolecular pump provided a base pressure of $\sim 10^{-9}$ torr for the evaporation chamber and differential ion pumps provided a base pressure of 5×10^{-10} torr for the analysis chamber. Crystals were loaded into the vacuum system from a loading cross and through the use of sample transfer probe; they could be transferred back and forth between the loading cross, the evaporation chamber and the analysis chamber. Surface analysis of the sample was made by Auger electron spectroscopy (AES) using a Physical Electronics system. To avoid specimen damage and atom desorption caused by excessively high current density, a beam current of 5 μA was used. Ar ion sputter etching was also used in order to obtain depth profiles of elemental composition.

After being polished and cleaned, the crystals were mechanically secured on to the sample stud by copper and stainless steel clips. As stated earlier, the two CdS crystals were mounted side by side with opposite sides (A and B faces) facing up to ensure the same treatments to both crystals. Auger spectra, collected on as-polished specimens, showed the presence of C, O_2 and Cl peaks as well as those of Cd and S. Because the polar surfaces of the CdS single crystals are not the cleavage surfaces of CdS, clean surfaces were produced by using 2 kV argon ion beam rastering on the surfaces to remove the contaminations followed by a 0.65 kV beam to anneal the crystals as described by Morimoto [18]. A set of spectra was collected on the clean surfaces before metal film deposition.

The crystals were then transferred to the evaporation chamber through the gate valve and the metal was evaporated on to them. The pressure of the evaporation chamber rose to 10^{-8} torr range during metal evaporation. A quartz crystal oscillator was used to monitor the thickness and the rate of metal film deposited. The crystals were then transferred back and forth between the analysis chamber and the evaporation chamber, as the thickness of the film was increased in steps up to 10 nm. The films were then sputtered off, in intervals, with the Ar ion beam. In order to ensure a uniform sputtering rate and to minimize surface damage and sputter-induced mixing effects, a 1 kV raster beam was used for this purpose. Auger spectra were collected at different time intervals, and depth profiles of elemental composition were obtained.

3. Results and discussion

A typical spectrum for an Al overlayer on CdS is shown in Fig. 1. A significant amount of O_2 is observed in this spectrum, an expected observation in view of the high stability of aluminium oxide. During the initial stages of Al film deposition, a broad Al $L\,M\,M$ peak appeared at 60 eV and then shifted to 68 eV at thicker film coverage. The low-energy (60 eV) peak became indiscernible when the film thickness reached about 1.5 nm on the A face and 3.0 nm on the B face, and a clear doublet was observed during the transition stage at a thickness of about 0.5–0.7 nm, as shown in Fig. 2a. The S peak did not show a significant position shift; however, its shape and intensity changed as shown in Fig. 2b. The Cd peak position shifted by about 2 eV toward a higher energy at about 0.5 nm thick Al film, as shown in Fig. 2c, and the shift increased in magnitude as the film became thicker.

The shift of the Al $L\,M\,M$ peak during the initial Al deposition can be attributed to the formation of aluminium sulphide with a charge transfer from Al to S. This is in agreement with previous studies with secondary X-ray photoelectron spectroscopy (SXPS) and LELS techniques [19, 20]. Considering the Auger Al peak shifts from 68–51 eV in Al_2O_3, the shift of 60 eV in this case corresponds to a less stable product relative to Al_2O_3, consistent with the higher electronegativity of O_2 relative to S. The compound may not be stoichiometric Al_2S_3 because of the intervention of
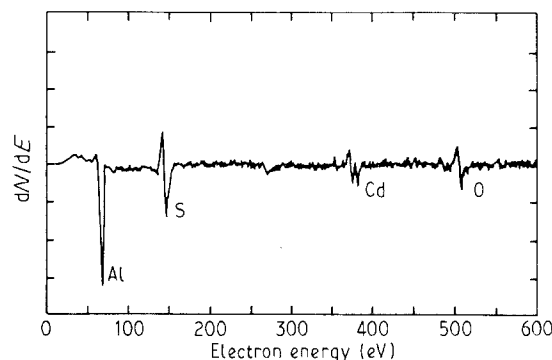

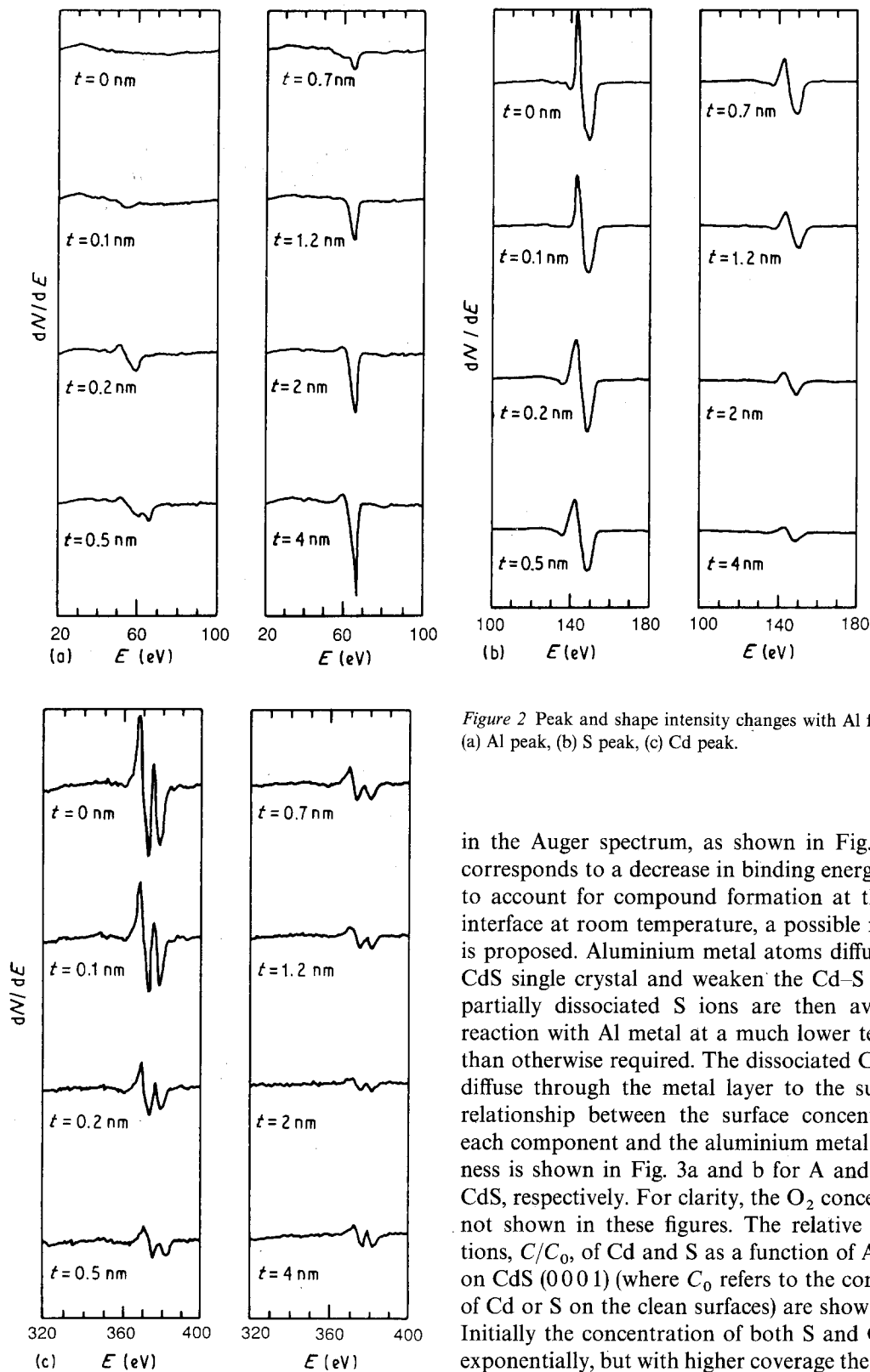*Figure 1* Typical Auger spectrum for Al on CdS.

1143

Figure 2 Peak and shape intensity changes with Al film thickness: (a) Al peak, (b) S peak, (c) Cd peak.

Cd atoms. No significant S spectral changes occur, because S anions remain strongly bonded. The initial appearance of only one chemically shifted Al LMM peak demonstrates that all the deposited Al reacted with the substrate CdS crystal and that a thin, continuous film was formed with no island formation. If islands of bulk metal were produced, both shifted and unshifted LMM features would appear.

The bonding of Al with S also promotes the dissociation of surface Cd atoms. This is evident from the slight shift of Cd MNN peak toward a higher energy

in the Auger spectrum, as shown in Fig. 2c, which corresponds to a decrease in binding energy. In order to account for compound formation at the Al–CdS interface at room temperature, a possible mechanism is proposed. Aluminium metal atoms diffuse into the CdS single crystal and weaken the Cd–S bonds, the partially dissociated S ions are then available for reaction with Al metal at a much lower temperature than otherwise required. The dissociated Cd can then diffuse through the metal layer to the surface. The relationship between the surface concentrations of each component and the aluminium metal film thickness is shown in Fig. 3a and b for A and B faces of CdS, respectively. For clarity, the O_2 concentration is not shown in these figures. The relative concentrations, C/C_0, of Cd and S as a function of Al coverage on CdS $(0\,0\,0\,1)$ (where C_0 refers to the concentration of Cd or S on the clean surfaces) are shown in Fig. 4. Initially the concentration of both S and Cd falls off exponentially, but with higher coverage the decrease is less dramatic. Because the metal film thicknesses are greater than the Auger electron escape depths of Cd and S at higher coverage, the observed concentrations of Cd and S are due to outdiffusion of these species. The outdiffusion is probably driven by the exothermic Al–S reaction.

The S/Cd concentration ratios increased rapidly during the initial metal film deposition up to a film thickness of about 0.5–1.0 nm and then dropped sharply to a value much smaller than 1, with the drop being much faster for the A face than for the B face, as shown in Fig. 5. The sharp increase of the S/Cd concentration ratio during the initial film deposition
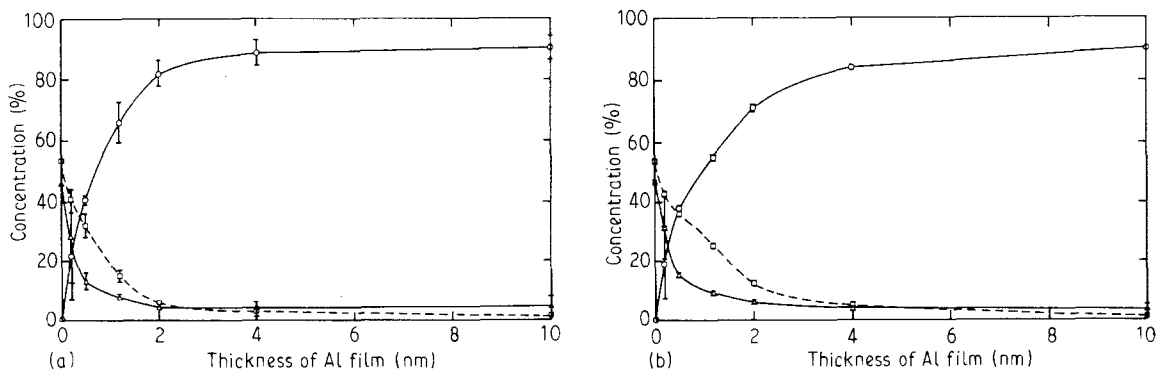
Figure 3 Surface concentrations of (○) Al, (□) S and (△) CdS as a function of Al coverage: (a) on (0 0 0 1) CdS, (b) on (0 0 0 $\bar{1}$) CdS.
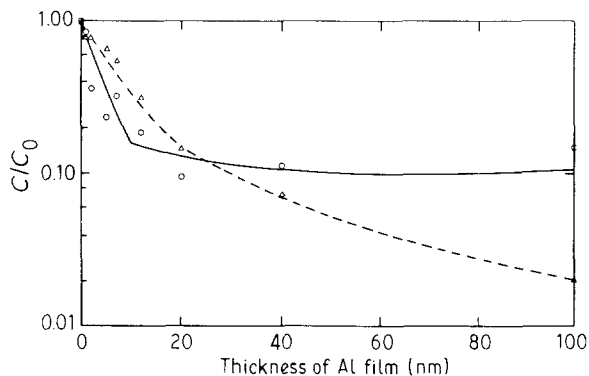

Figure 4 Relative concentrations of (○) Cd and (△) S as a function of Al coverage on (0 0 0 1) CdS.
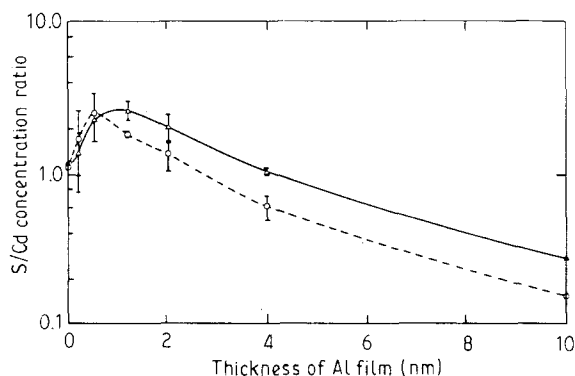

Figure 5 S/Cd concentration ratios as a function of Al film thickness.

(up to about 1.0 nm) may be due to the reactive sulphur outdiffusion at the metal–semiconductor interface. The chemical reaction between Al and S draws the anion toward the free metal surface. This "chemical drawing" of the S anions coupled with the slower cation outdiffusion through the reacted layer, may account for the large concentration difference of anion and cation in the metal overlayer at a thickness of 0.5–1.0 nm at room temperature. It has been implied by Brillson [21] that this phenomenon is induced by the dipole voltage formed at the Al–CdS interface.

Considering the dipole field induced when the Al film was deposited on to the CdS crystal and assuming that the surface charge is the same in prismatic plane and basal planes, the positive dipole of 0.21 eV for the

interface between Al and CdS (1 0 $\bar{1}$ 0) measured by Brillson [3] would be modified by the field due to the polarity of the polar surfaces. The net effect is an increase in the total field strength in the Cd surface and a decrease in the S surface. Because the positive dipole enhances the outdiffusion of S and retards the outdiffusion of Cd, a S/Cd concentration ratio greater than 1 is expected on both sides of the crystal, with a higher ratio on the Cd surface than on the S surface. The S/Cd concentration ratio was expected to increase continuously as the film thickness increased, as was observed by Brillson *et al.* [22] in the similar case of CdSe. However, the rapid decrease of the ratio after the first few atomic layers in our study suggests that the anions are chemically trapped and localized preferentially near the interface. The electromigration induced by the dipole voltage may have only a short-range effect and chemical trapping dominates at longer distances.

No significant difference in S/Cd concentration ratio was found between the two opposite {0 0 0 1} polar surfaces during initial deposition of Al, indicating the possibility that the extrinsic metal–semiconductor dipole is much stronger than the intrinsic dipole induced by the surface polarity and surface charge. An alternative explanation is that neither one of the dipole fields played an important role in semiconductor outdiffusion.

At high metal coverage, due to the strong chemical trapping effect, the S/Cd concentration ratio becomes much smaller than 1. From the different film thicknesses required to change the energy positions of the Al peak from reacted to bulk metal between the polar surfaces, a larger interface width on the S face can be obtained, i.e. a thicker "reacted" layer on the S face. This indicates a weaker chemical trapping effect and a larger S/Cd concentration ratio on the S surface, in agreement with our observations. The difference in interface thicknesses between the polar surfaces can be explained by the different stabilities of the polar surfaces. Experimental evidence has been provided to suggest that the S face was much less stable structurally and chemically than the Cd face [23], therefore, a broader interface was expected. This, however, is in apparent contradiction with vapour pressure observations in which the Cd face exhibited a higher evaporation rate [24]. However, surface charge is believed to play a dominant role in the evaporation process while
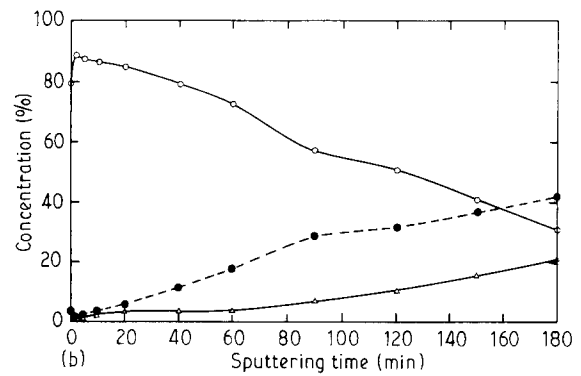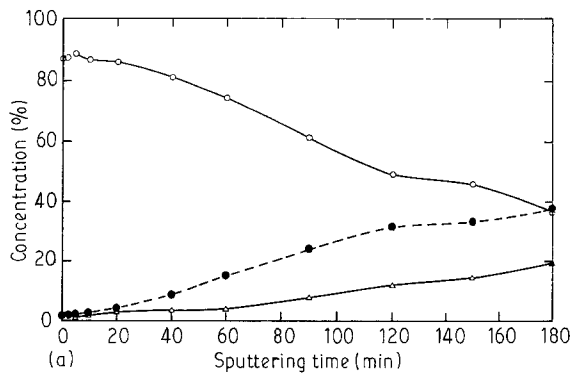
Figure 6 Surface concentrations of (○) Al, (●) S and (△) CdS as a function of sputtering time: (a) on (0 0 0 1) CdS, (b) on (0 0 0 $\bar{1}$) CdS.
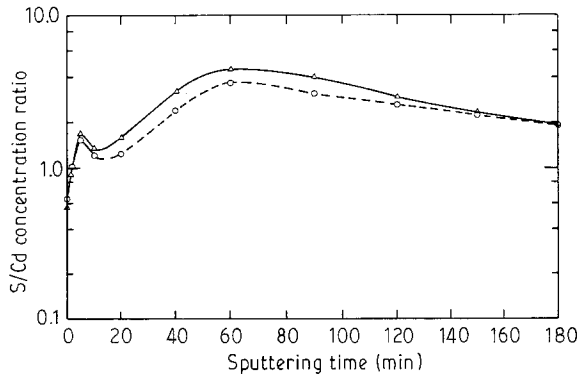

Figure 7 S/Cd concentration ratios as a function of sputtering time. (○) A face, (△) B face.

it may not be significant in the process of metal–semiconductor interdiffusion.

Sputter depth profiles on A and B CdS surfaces are shown in Fig. 6a and b, respectively. By integrating the area under the Al concentration curve as a function of sputtering time, the average sputtering rate was estimated to be ~ 0.071 nm min^{-1}. The S/Cd concentration ratios for these two cases are shown in Fig. 7. The ratios increased rapidly during the initial sputtering process, and decreased somewhat in the region below the surface and then increased as the metal–semiconductor interface was approached. The ratios were greater than 1 throughout the metal overlayer, and reached a maximum at about 4.0 nm from the surface then gradually decreased toward the bulk ratios as the metal layers were completely removed. The initial increase of the S/Cd concentration ratio during sputtering is in agreement with the slow S diffusion as discussed above. Splitting and shifting of the aluminium peak appeared at about 6.0 nm from the surface (4.0 nm from the original interface) as shown in Fig. 8a. Another sample in which the sputtering process started at 4.0 nm thick Al film is shown in Fig. 8b. Here the peak splitting and shifting can be more easily
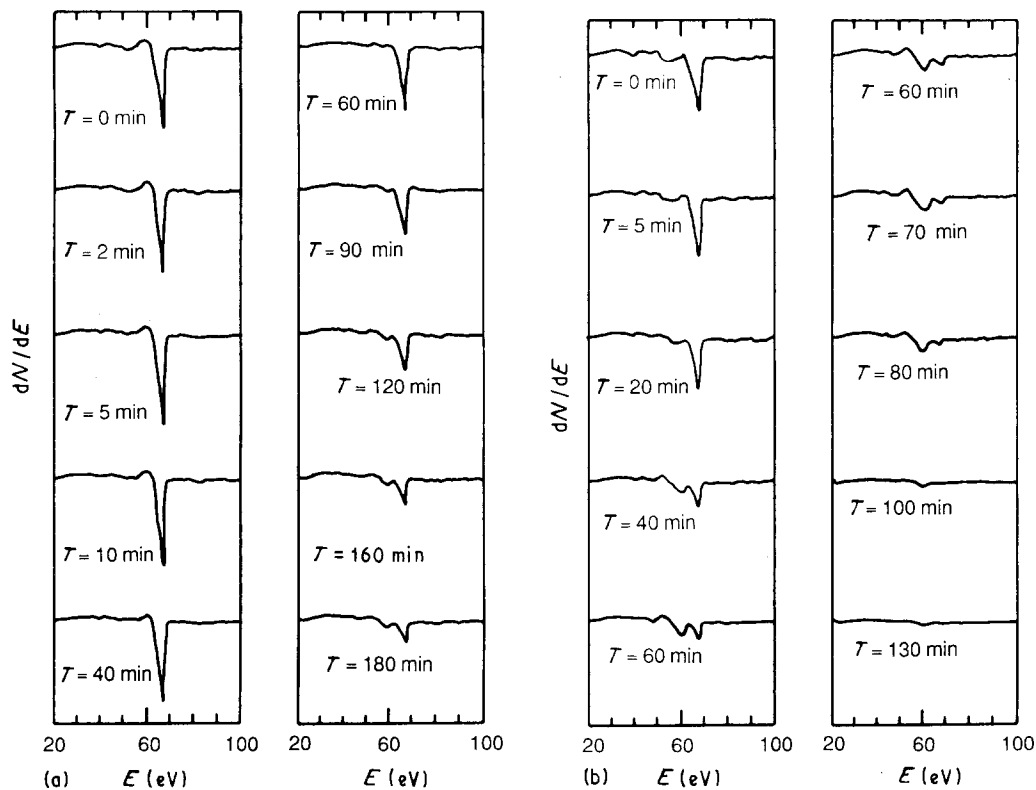

Figure 8 (a) Al peak shape and intensity as a function of sputtering time. (b) As (a) but sputtering started at 4.0 nm thick Al film.
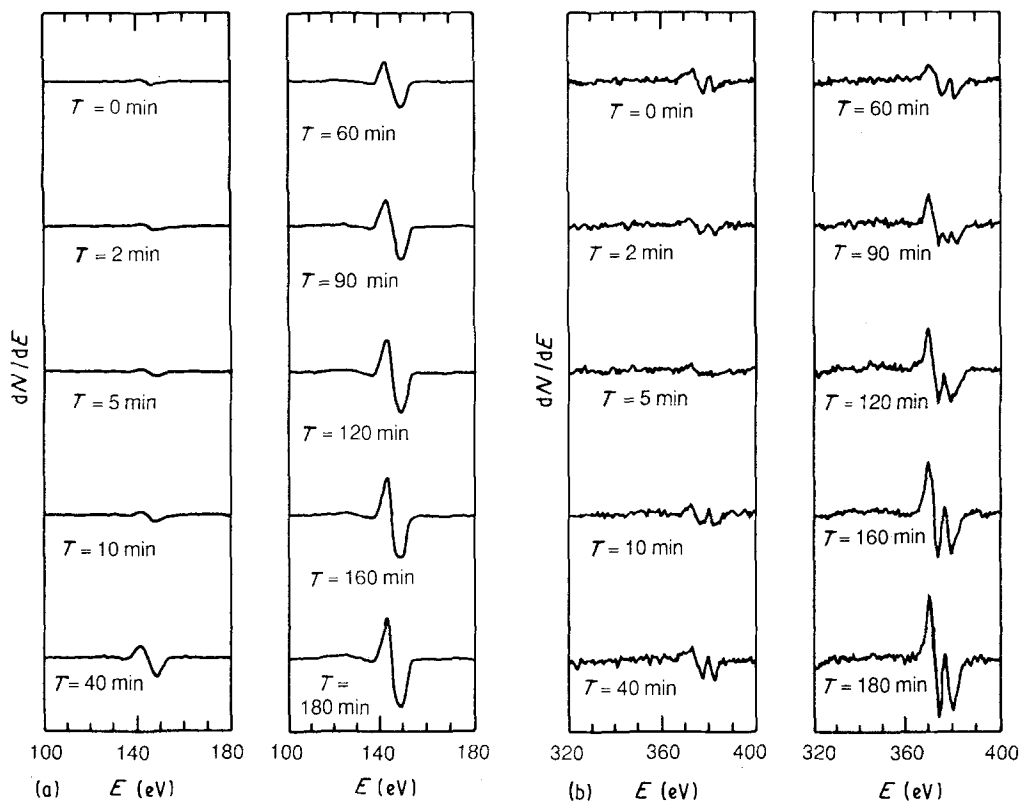
Figure 9 Peak shape and intensity as a function of sputtering time: (a) S peak, (b) Cd peak.

identified. Because the reacted Al peak disappeared at a thickness of about 2.0 nm during the film deposition process, it can be assumed that although a highly localized reaction was produced at the Al–semiconductor interface, the reacted layer continued to grow at room temperature. The maximum value of the S/Cd concentration ratio was observed before the Al peak splitting and shifting, implying that the S ions are trapped at the boundary between metal Al and the reacted (Al–S) layer. This suggests that S anions slowly diffuse through the reacted layer, but once they reach the Al–"AlS" boundary, they could rapidly diffuse to the surface by the "chemical drawing" effect.

From the depth profiles in Fig. 6a and b, it can be seen that large amounts of Al are still present even after 3 h sputter etching. Both reacted and unreacted Al peaks extended into the bulk of the CdS crystal. The S peak, as shown in Fig. 9a, did not exhibit any peak shifting, although it had not regained its characteristic shape observed in pure CdS crystal. These observations indicate that Al penetrates past the interface into the substrate CdS crystal and reacts with S to form a chemical compound. The cadmium peak exhibited a clear splitting and shifting after about 6.0 nm thick films were removed from the surface as shown in Fig. 9b. This confirmed that the dissociation of Cd is the result of the formation of the aluminium chalcogenide.

4. Conclusions

1. Al reacts strongly with CdS causing a chemical shift of the Al Auger peaks. A chemical drawing effect dominates at low coverage while a chemical trapping effect dominates at longer distances.

2. A sharp boundary was formed initially between Al and CdS due to the chemical trapping effect; however, due to the reactive outdiffusion, the boundary may extend over tens of nanometres.

3. A possible mechanism is proposed to explain the change of outdiffusion stoichiometry in the Al–CdS system. The S anions are chemically drawn to the free metal surface initially with a very fast diffusion rate, the supply of the S anions may be limited as the thickness of the reacted interface increased. This mechanism indicates that both "chemical trapping" and "chemical drawing" are the same process, and it can be used to explain metal–semiconductor interfaces for both III–V and II–VI compounds.

4. The chemical bonding at the microscopic interface plays a central role in the process of interdiffusion. The lack of consistency between measurements made here and those reported elsewhere may be due to differences in crystal orientation and surface preparation.

Acknowledgement

References

1. L. J. BRILLSON, *J. Phys. Chem. Solids* **44** (1983) 703.
2. *Idem, Surf. Sci. Rep.* **2** (1982) 123.
3. *Idem, J. Vac. Sci. Technol.* **16** (1979) 1137.
4. *Idem, Phys. Rev.* **B18** (1978) 2431.
5. C. F. BRUCKER and L. J. BRILLSON, *J. Vac. Sci. Technol.* **18** (1981) 787.

6. L. J. BRILLSON, *ibid.* **15** (1978) 1378.
7. *Idem, Phys. Rev. Lett.* **40** (1978) 260.
8. L. J. BRILLSON, C. F. BRUCKER, N. G. STOFFEL, A. D. KATNANI and G. MARGARITONDO, *ibid.* **46** (1981) 838.
9. A. N. MARIANO and R. E. HANNEMAN, *J. Appl. Phys.* **34** (1963) 384.
10. V. KUMAR and F. A. KROGER, *J. Solid State Chem.* **3** (1971) 387.
11. G. H. HERSHMAN and F. A. KROGER, *ibid.* **2** (1970) 483.
12. N. K. ABRIKOSOV, V. F. BANKINA, L. V. PORETS-KAYA, L. E. SHELIMOVA and E. V. SKUDNOVA, "Semi-conducting II–VI, IV–VI, and V–VI Compounds" (Plenum Press, New York, 1969) p. 29.
13. J. FRENKEL, "Kinetic Theory of Liquids" (Clarendon Press, Oxford, 1946).
14. H. C. GATOS, *J. Appl. Phys.* **32** (1961) 1232.
15. E. K. CHIEH and Z. A. MUNIR, to be published.
16. I. V. SAMARASEKERA and Z. A. MUNIR, *High Temp. Sci.* **10** (1978) 155.
17. E. P. WAREKOIS, M. C. LAVINE, A. N. MARIANO and H. C. GATOS, *J. Appl. Phys.* **33** (1962) 690.
18. J. MORIMOTO, *Jpn Mem. Nat. Defense Acad.* **20** (1980) 97.
19. L. J. BRILLSON, R. S. BAUER, R. Z. BACHRACH and J. C. McMENAMIN, *J. Vac. Sci. Technol.* **17** (1980) 476.
20. L. J. BRILLSON, *Phys. Rev. Lett.* **38** (1977) 245.
21. *Idem, J. Vac. Sci. Technol.* **20** (1982) 652.
22. L. J. BRILLSON, C. F. BRUCKER, A. D. KATNANI, N. G. STOFFEL, R. DANIELS and G. MARGARITONDO, *Surf. Sci.* **132** (1983) 212.
23. S. C. CHANG and P. MARK, *J. Vac. Sci. Technol.* **12** (1975) 629.
24. R. B. LEONARD and A. W. SEARCY, *J. Appl. Phys.* **42** (1971) 4047.